Regulation of vascular endothelial growth factor receptor 2 trafficking and angiogenesis by Golgi localized t-SNARE syntaxin 6

Venkatraman Manickam,[1] Ajit Tiwari,[1] Jae-Joon Jung,[1] Resham Bhattacharya,[2] Apollina Goel,[3] Debabrata Mukhopadhyay,[2] and Amit Choudhury[1]

[1]Department of Anatomy and Cell Biology, University of Iowa, Iowa City, IA; [2]Department of Biochemistry and Molecular Biology, Mayo Clinic College of Medicine, Rochester, MN; and [3]Free Radical and Radiation Biology Program, Department of Radiation Oncology, University of Iowa, Iowa City, IA

Vascular endothelial growth factor receptor 2 (VEGFR2) plays a key role in physiologic and pathologic angiogenesis. Plasma membrane (PM) levels of VEGFR2 are regulated by endocytosis and secretory transport through the Golgi apparatus. To date, the mechanism whereby the VEGFR2 traffics through the Golgi apparatus remains incompletely characterized. We show in human endothelial cells that binding of VEGF to the cell surface localized VEGFR2 stimulates exit of intracellular VEGFR2 from the Golgi apparatus. Brefeldin A treatment reduced the level of surface VEGFR2, confirming that VEGFR2 traffics through the Golgi apparatus en route to the PM. Mechanistically, we show that inhibition of syntaxin 6, a Golgi-localized target membrane-soluble N-ethylmaleimide attachment protein receptor (t-SNARE) protein, interferes with VEGFR2 trafficking to the PM and facilitates lysosomal degradation of the VEGFR2. In cell culture, inhibition of syntaxin 6 also reduced VEGF-induced cell proliferation, cell migration, and vascular tube formation. Furthermore, in a mouse ear model of angiogenesis, an inhibitory form of syntaxin 6 reduced VEGF-induced neovascularization and permeability. Our data demonstrate the importance of syntaxin 6 in the maintenance of cellular VEGFR2 levels, and suggest that the inhibitory form of syntaxin 6 has good potential as an antiangiogenic agent. (*Blood*. 2011;117(4):1425-1435)

Introduction

Members of the vascular endothelial growth factor (VEGF) family bind to cell-surface receptors to regulate both physiologic and pathologic angiogenesis.[1] The activities of the VEGF-A isoform are mediated primarily through its interactions with 2 high-affinity receptor tyrosine kinases expressed on the vascular endothelium: VEGF receptor 2 (VEGFR2, KDR, Flk-1) and VEGFR1 (Flt-1).[2] VEGF-mediated angiogenic signaling has been attributed primarily to the signal transduction processes that are initiated by VEGFR2.[3] Cell-surface VEGFR2 internalized by the clathrin-dependent endocytic process is constitutively recycled back to the plasma membrane (PM).[4-7] Upon VEGF stimulation a fraction of the internalized endocytic pool of VEGFR2 is sorted toward late endosomes and lysosomes for degradation, whereas the remainder is recycled to the PM.[4,5,8-10] Antiangiogenic approaches currently in use work by blocking VEGF binding to VEGFR2 and/or signaling by the receptor tyrosine kinases.[11] These strategies highlight the importance of intracellular transport mechanisms that coordinate the expression of VEGFR2 at distinct subcellular locations.

The Golgi apparatus is a central hub for membrane trafficking across the mammalian cell. It receives newly synthesized proteins and lipids from the endoplasmic reticulum (ER), modifies many of these cargoes as they pass through, and finally sorts them to various destinations as they exit.[12-15] Thus the Golgi apparatus is a likely candidate for regulating VEGFR2 trafficking. Unraveling the precise transport pathway and the molecular players may offer better understanding of regulation of the VEGFR2 function. Nevertheless, to date it remains unclear how secretory transport through the Golgi apparatus coordinates the cell-surface expression of VEGFR2.

In eukaryotic cells, most membrane fusion steps require soluble *N*-ethylmaleimide–sensitive factor attachment protein receptors (SNAREs).[16,17] The SNAREs are classified into 2 major classes based on the presence of a glutamine (Q SNAREs or t-SNAREs) or an arginine (R SNAREs or v-SNAREs) in the center of the SNARE motif.[16] Syntaxin 6, syntaxin 10, and syntaxin 16 are members of the t-SNARE protein family, and are localized primarily in the Golgi apparatus but also in endosomes, and are involved in the transport of molecules to and from the Golgi apparatus.[18-23] Previously, we showed that syntaxin 6 regulates the post-Golgi transport of membrane microdomain components to the PM.[18] However, to date the SNARE complex that mediates VEGFR2 trafficking remains unidentified.

In the current study, we investigated the possibility that syntaxin 6 affects the post-Golgi transport and cell-surface levels of VEGFR2, as well as VEGF-induced angiogenesis. We show that in quiescent endothelial cells a pool of VEGFR2 is present in the Golgi apparatus, and that this Golgi pool of VEGFR2 is rapidly depleted in response to stimulation with VEGF. Among syntaxin 6, syntaxin 10, and syntaxin 16, syntaxin 6 was found to maintain cellular levels of the VEGFR2. When syntaxin 6 function was selectively inhibited, VEGFR2 was targeted to lysosomes for degradation, and the levels of VEGF-induced proliferation, migration, and morphogenesis were decreased. These results show for the first time that syntaxin 6 regulates post-Golgi trafficking of

Submitted June 21, 2010; accepted November 3, 2010. Prepublished online as *Blood* First Edition paper, November 9, 2010; DOI 10.1182/blood-2010-06-291690.

The online version of this article contains a data supplement.

The publication costs of this article were defrayed in part by page charge payment. Therefore, and solely to indicate this fact, this article is hereby marked "advertisement" in accordance with 18 USC section 1734.

VEGFR2 as well as VEGF-induced angiogenic processes. Furthermore, expression of an inhibitory form of syntaxin 6 was found to block VEGF-induced angiogenesis, providing the first demonstration that an inhibitory mutant t-SNARE can act as a potent antiangiogenic agent.

Methods

Reagents

The rabbit monoclonal antibody (mAb) against human VEGFR2 (55B11) was purchased from Cell Signaling Technology. The goat anti–human VEGFR2 antibody, goat anti–human VEGFR1 antibody, and recombinant VEGF-A_{165} (VEGF) were purchased from R&D Systems. The goat polyclonal antibody (pAb) against syntaxin 6 and the rabbit polyclonal antibody against VEGFR1 were obtained from Santa Cruz Biotechnology. The mAb against lysosome-associated membrane protein 2 (Lamp2) was obtained from the Developmental Studies Hybridoma Bank at the University of Iowa. The mAbs against early endosome-associated antigen 1 (EEA1), syntaxin 6, and trans-Golgi network 46 (TGN46), the rat anti–mouse CD31 antibody, and growth factor–reduced Matrigel were obtained from BD Biosciences. Recombinant adenovirus expressing the cytosolic inhibitory form of syntaxin 16 (syntaxin 16-cyto) was a gift from Dr Gwyn W. Gould (University of Glasgow). Rabbit pAb against syntaxin 6 and syntaxin 16 and mouse mAb against syntaxin 16 were purchased from Synaptic Systems. Fugene 6 HD transfection reagent, protease inhibitor, and phosphatase inhibitor cocktail tablets were obtained from Roche Diagnostics. Alexa Fluor–conjugated secondary Abs were obtained from Invitrogen, Molecular Probes. Vectashield mounting medium was purchased from Vector Laboratories. The mAbs against α-tubulin, cycloheximide (CHX), chloroquine (CHQ), bafilomycin AI (Baf), and lactacystin (Lac) were purchased from Sigma-Aldrich. Protein A and protein G Sepharose beads and Amplify-fluorographic Reagent were purchased from GE Healthcare. SuperSignal West Femto ECL reagent was obtained from Thermo Scientific. ^{35}S-methionine and cysteine (EasyTag Express ^{35}S Protein labeling mix) were obtained from PerkinElmer.

Cell culture

Primary human umbilical vein endothelial cells (HUVECs) were obtained from Lonza and cultured on collagen-coated plates in complete medium (endothelial cell basal medium containing supplements from Lonza). HUVECs were used only between passages 3 and 7. The 293T human embryonic kidney cells with simian virus 40 large T antigen (ATCC) were maintained in Dulbecco modified minimum essential medium containing 10% fetal bovine serum. Treatment with VEGF-A_{165} was carried out at 50 ng/mL concentrations unless otherwise indicated.

Adenoviral infections, plasmids, and short interfering and short hairpin RNAs

Recombinant adenovirus expressing the cytosolic domains of syntaxin 6 and syntaxin 16 (designated syntaxin 6–cyto and syntaxin 16–cyto) were used as described previously.[18,24] Except as noted, cells were infected at shown with the indicated adenovirus (titer $\sim 1.5 \times 10^7$ plaque-forming units/mL) at a multiplicity of infection of 1:75 in serum-free cell-culture medium. After 12 hours of infection, the medium was replaced with normal medium supplemented with 10% serum, and the cells were used for the experiments 12 to 24 hours later. We cloned both full-length human *STX10* (residues 1-249) and a cytosolic form (residues 1-228) into the enhanced green fluorescence protein (EGFP) plasmid vector pEGFP-C1 (Clontech); the expected sequence (NM_003765) for each construct was confirmed. EGFP-syntaxin 10 was used for cellular localization studies.

RNA interference–mediated knockdown was performed using Silencer Select predesigned short interfering RNAs (siRNAs) against *STX6* (5′-GCAACUGAAUUGAGUAUAA-3′) and *STX16* (5′-CAGCGAUUGGUGUGACAAA-3′) in conjunction with the siPORT NeoFX transfection reagent from Ambion. The specificity and extent of knockdown of both proteins was determined 24, 48, and 72 hours after transfection of 293T cells, by immunoblotting. In the case of 293T cells, both syntaxin 6 and syntaxin 16 were reduced by approximately 90% at the protein level (data not shown). RNA interference was less successful in HUVECs, which are less transfectable; the fraction of cells showing at least a 10-fold reduction in syntaxin 6 or syntaxin 16 levels after transfection was approximately 12% to 15%, as judged by immunofluorescence (supplemental Figure 5, available on the *Blood* Web site; see the Supplemental Materials link at the top of the online article).

Subcellular fractionation

Details of the fractionation protocol are described in supplemental Methods.

Immunoblotting, immunoprecipitation, and ^{35}S-methionine metabolic labeling

Procedures for labeling protocol are described in supplemental Methods.

Cell-surface biotinylation studies

Measurements of the cell surface–localized pool of biotinylated VEGFR2 and intracellular degradation of this population were performed using methods previously described.[10] Details of cell-surface biotinylation measurements are provided in supplemental Methods.

Internalization and degradation of surface VEGFR2

The internalization of VEGFR2 from the cell surface and its degradation were analyzed using previously described methods.[25] We used an E-tagged single chain fragment variable (ScFv) mAb against the extracellular domain of human VEGFR2 (ScFvA7), which has been reported to be devoid of biologic activity.[25,26] Cells were maintained at 10°C (a temperature at which endocytosis does not occur)[27] with 10 μg/mL of antibody in Hanks minimum essential medium (HMEM) buffer ([pH 7.4], 13.8mM HEPES acid, 137mM NaCl, 5.4mM KCl, 5.5mM glucose, 2.0mM glutamine, 0.4mM KH_2PO_4, 0.18mM Na_2HPO_4, 1.25mM $CaCl_2$, and 0.08mM $MgSO_4$) for 30 minutes. Before stimulation with VEGF, cells were washed in ice-cold HMEM buffer with 1% BSA to remove unbound Ab, and maintained in fresh buffer. Cells were then incubated with VEGF at 10°C for an additional 30 minutes to allow VEGF to bind to surface VEGFR2. Samples were then incubated at 16°C for 30 minutes in HMEM buffer as previously described, to allow internalized VEGF-VEGFR2 complexes to accumulate in early endosomes.[27] Subsequently, samples were moved to a cold station maintained at 10°C, and the remaining surface-bound antibody was removed by an acid wash (3 washes with ice-cold 50mM glycine in HMEM buffer [pH 2.5] and 2 washes with HMEM buffers [pH 7.5]). The cells were then subjected to a chase at 37°C in HMEM buffer. At each of several time points, the cells were moved to a 10°C cold station and were acid washed to remove any antibody that may have recycled to the surface during the chase. To assess the intracellular distribution of the anti-VEGFR2 antibody, cells were fixed, permeabilized, and incubated with fluorescein isothiocyanate (FITC)–labeled rabbit antibody against its E-tag. Samples were then processed for fluorescence microscopy.

Microscopy and image analysis

For immunofluorescence studies, cells were grown on acid-washed glass coverslips. Cells were fixed, permeabilized, and then labeled with primary antibodies. Microscopy and image analysis are described in supplemental Methods.

Assays

Endothelial cell proliferation, migration, and vascular tube formation assays are conducted. Detailed protocols for HUVECs proliferation, wound healing, Boyden chamber migration, and Matrigel-based morphogenesis assays are provided in supplemental Methods.

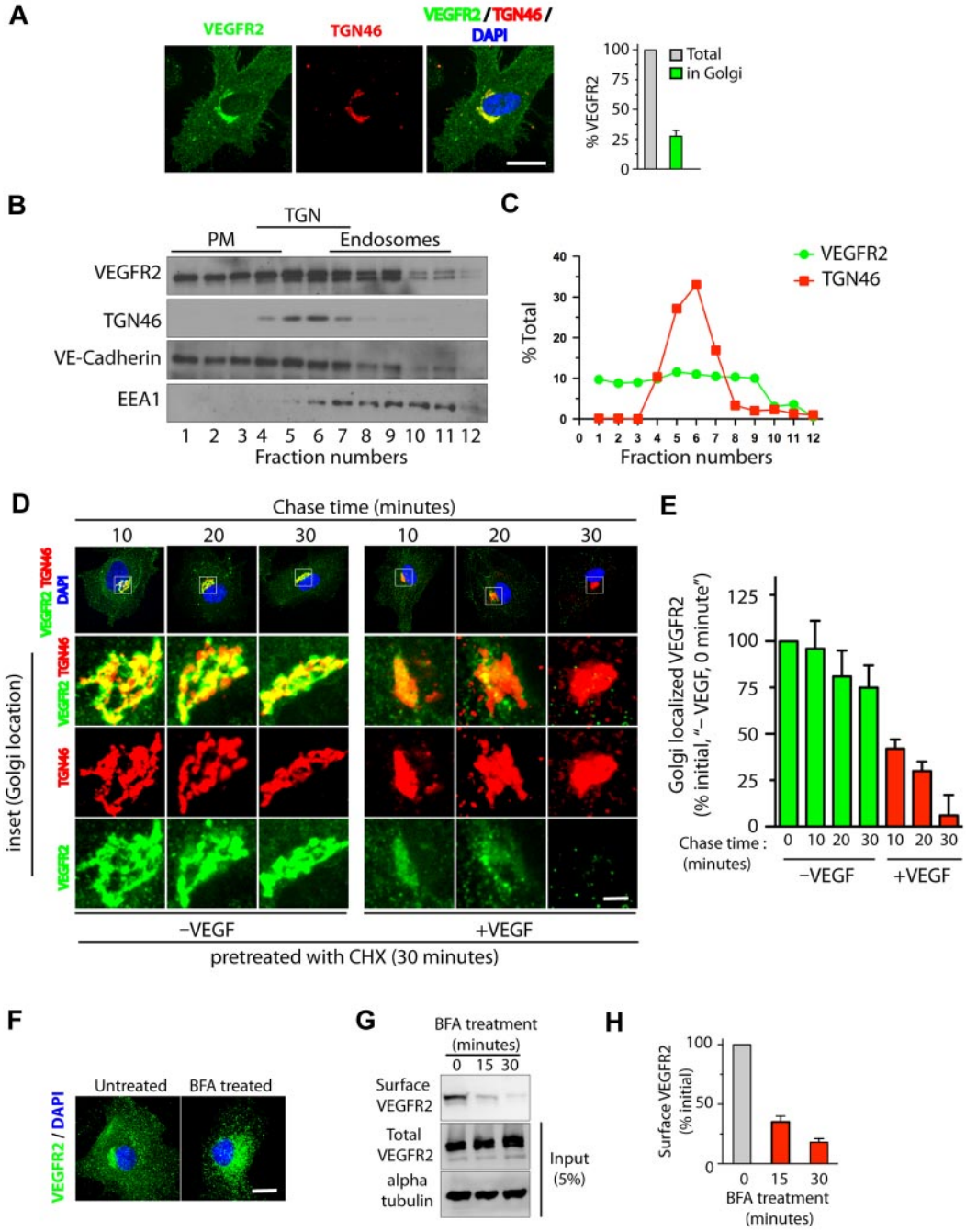

Figure 1. VEGF stimulates exit of VEGFR2 from the trans-Golgi complex. (A) Serum-starved HUVECs were labeled with mAb against VEGFR2 (55B11) and TGN46 (Golgi marker). Total cell-associated and Golgi-localized fluorescence intensity of VEGFR2 was quantified by image analysis. Values are expressed as a fraction of the total VEGFR2 in the Golgi apparatus. (B) Homogenates prepared from serum-starved HUVECs were fractionated on a self-generated Optiprep gradient (10%, 20%, 30%) and immunoblotted with antibodies against proteins enriched in the PM (vascular endothelial-Cadherin); the trans-Golgi complex (TGN46); or endosomes (EEA1). (C) Percentage of total VEGFR2 and TGN46 in each fraction, based on quantification of density of bands in each fraction obtained by Optiprep gradient centrifugation. (D) Effects of VEGF-A treatment on VEGFR2 localization at the Golgi apparatus. Serum-starved HUVECs were treated with CHX (10 μg/mL), and immunofluorescence imaging was carried out for VEGFR2 and TGN46 localization. (E) Quantification of the Golgi-localized VEGFR2 (overlapping with TGN46) shown in panel D. Values are expressed as a percentage of change in intensity of Golgi-localized VEGFR2 signal (relative to initial intensity in at 0 minutes chase at 37°C, data not shown). Percentages in panels A and E represent mean (± SD) in n = 90 cells for each condition from 5 separate experiments. For panel E, $P \leq .05$. (F-G) Effects of BFA treatment on VEGFR2 transport in HUVECs. (F) Representative images of immunofluorescence analysis of untreated and BFA-treated cells stained with VEGFR2 antibody are shown. (G) Biotinylation-based analysis of cell-surface VEGFR2. Surface proteins labeled with the biotinylation reagent sulfo-NHS-SS–biotin were pulled down with streptavidin-Sepharose, and 5% of the total cell lysate and biotinylated cell-surface protein was separated by sodium dodecyl sulfate polyacrylamide gel electrophoresis followed by Western blot analysis with antibody against VEGFR2. (H) Quantification of band density for the cell-surface VEGFR2. Percentage is expressed as the change in surface VEGFR2 after BFA treatment (relative to initial levels). The percentage represents mean (± SD) for n = 3 and $P \leq .05$. Scale bar represents 5 μm.

Animal care and angiogenesis assay

All animal studies were approved by The University of Iowa Animal Care Committee and The Mayo Clinic and Foundation Institutional Animal Care Use Committee. Studies were carried out in accordance with the principles and procedures outlined in the National Institutes of Health (NIH) guidelines for the care and use of experimental animals. Mice (Nu/Nu, 6-8 weeks of age; Charles River Laboratories) under anesthesia were injected with the indicated recombinant adenoviruses as previously described.[28,29]

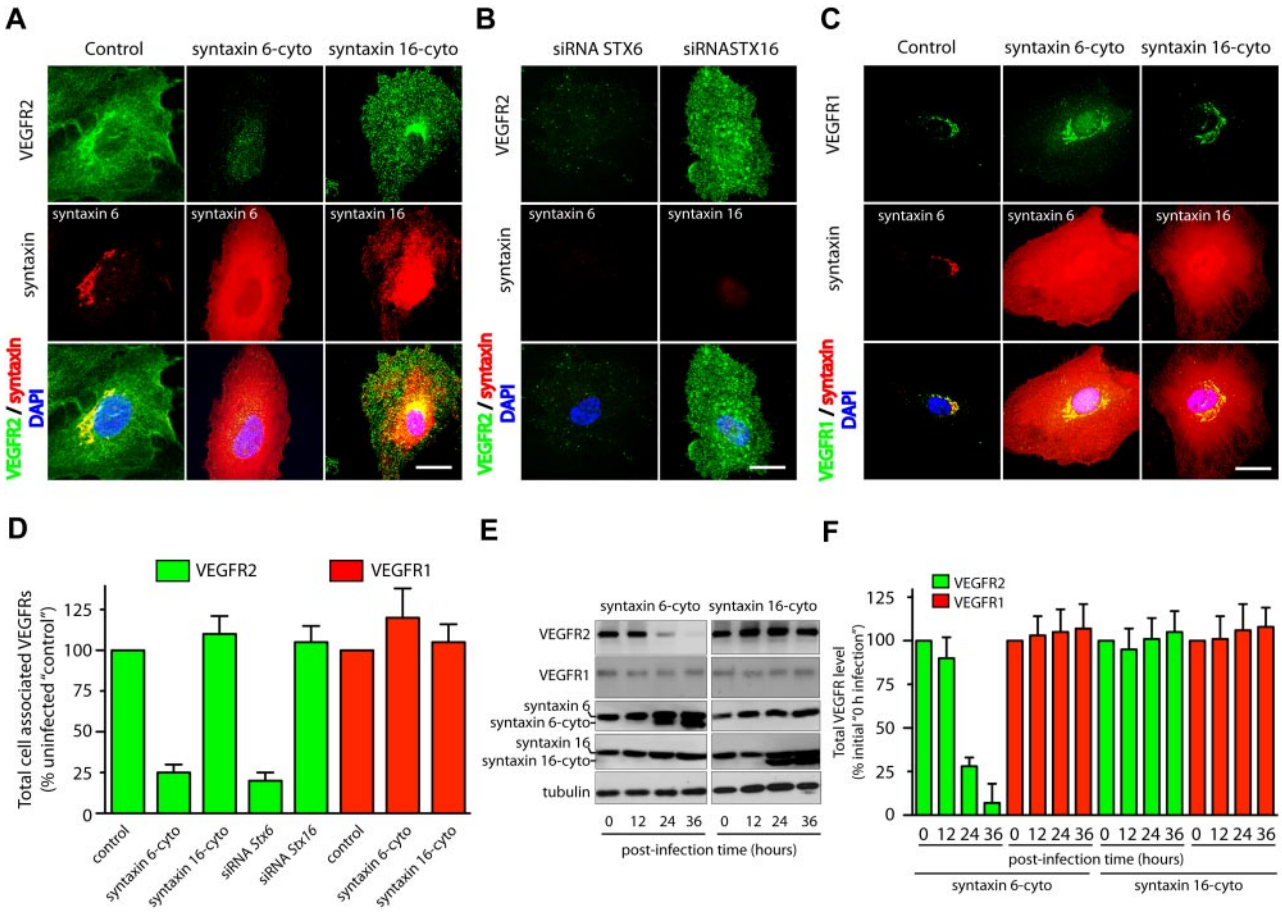

Figure 2. Inhibition of syntaxin 6 function decreases the levels of VEGFR2 but not the levels of VEGFR1. (A,D) Uninfected (Control) and syntaxin 6-cyto or syntaxin 16-cyto expressing HUVECs (after 20 hours of infection) were stained with mAb against VEGFR2 (55B11), syntaxin 6 (in Control and syntaxin 6-cyto–treated cells) or syntaxin 16 (in syntaxin 16-cyto–treated cells). Samples were then fixed and observed under fluorescence microscope. (B) HUVECs were subjected to siRNA-mediated syntaxin 6 or syntaxin 16 knockdown, and immunostained for VEGFR2. Representative images showing staining for intracellular VEGFR2 in cells in which endogenous syntaxin 6 or syntaxin 16 was knocked-down over 90% after 72 hours of siRNA treatment. (C) Samples were fixed and observed as in panel A, but stained with goat pAb against VEGFR1 and antibodies against syntaxin 6 or syntaxin 16. (D) Quantification of intracellular VEGFR2 or VEGFR1 in syntaxin 6-cyto and syntaxin 16-cyto expressing cells, and in cells in which endogenous syntaxin was knocked down by siRNA treatment (as in panels A-C). Epifluorescence images were acquired and total cell-associated fluorescence was quantified by image analysis. Values represent relative change in the levels of VEGFR2 or VEGFR1 normalized to an arbitrary value of 100 for untreated controls. Percentage is expressed as mean (± SD) of n = 90 cells for each condition from 3 separate experiments; $P \leq .001$. (E) Lysates were prepared from uninfected, syntaxin 6-cyto– or syntaxin16-cyto–infected HUVECs (after infection for various periods of time, as indicated) and samples were immunoblotted for VEGFR2 (55B11) and VEGFR1 (rabbit polyclonal). Relative level of endogenous syntaxin 6, syntaxin 16, or tubulin in cell lysate is shown. (F) VEGFR2 and VEGFR1 band density from panel E was quantified and results represent relative levels of VEGFR2 and VEGFR1 after normalization to an arbitrary value of 100 for 0 minutes after infection. Percentage is expressed as mean (± SD) for n = 3; $P \leq .005$). Scale bar represents 5 μm.

Details on the mouse ear angiogenesis assay, the preparation of mouse ear extracts, immunohistochemistry, and the vascular permeability assay are provided in supplemental Methods.

Statistical analysis

All values are expressed as mean (± SD). Statistical significance was determined using 2-sided Student *t* test with GraphPad Prism Version 4.0 software. A value of $P < .05$ was considered significant unless stated otherwise.

Results

VEGF stimulates VEGFR2 to exit the trans-Golgi compartment

Quantitative epifluorescence-based imaging of the cellular distribution of VEGFR2 in HUVECs revealed that approximately 25% to 30% of total VEGFR2 colocalizes with the trans-Golgi marker TGN46 (Figure 1A). Consistent with these findings, Optiprep gradient fractionation resulted in 30% to 40% of the total VEGFR2 cofractionating with TGN46 (Figure 1B-C). We next examined whether stimulation with VEGF affects the trafficking of VEGFR2 from the trans-Golgi compartment. For this, serum-starved HUVECs pretreated with CHX were incubated for 1 hour at 20°C to enrich VEGFR2 at the Golgi. Cells were then treated with VEGF (in the presence of CHX) for different times, and colocalization of VEGFR2 with the Golgi was monitored. A rapid loss of VEGFR2 from the Golgi compartment (95% within 30 minutes of VEGF stimulation) relative to that in unstimulated cells (25% over the same period) was observed (Figure 1D-E). These results suggest that VEGFR2 localizes in Golgi and stimulation with VEGF mobilizes VEGFR2 from the Golgi compartment.

Syntaxin 6 is a trans-Golgi and endosome-localized SNARE protein and facilitates trans-Golgi and post-Golgi vesicle fusion processes (supplemental Figure 2).[30,31] We next investigated whether stimulation with VEGF leads to altered localization of syntaxin 6 in relation to VEGFR2. Indeed, VEGF stimulation led to a

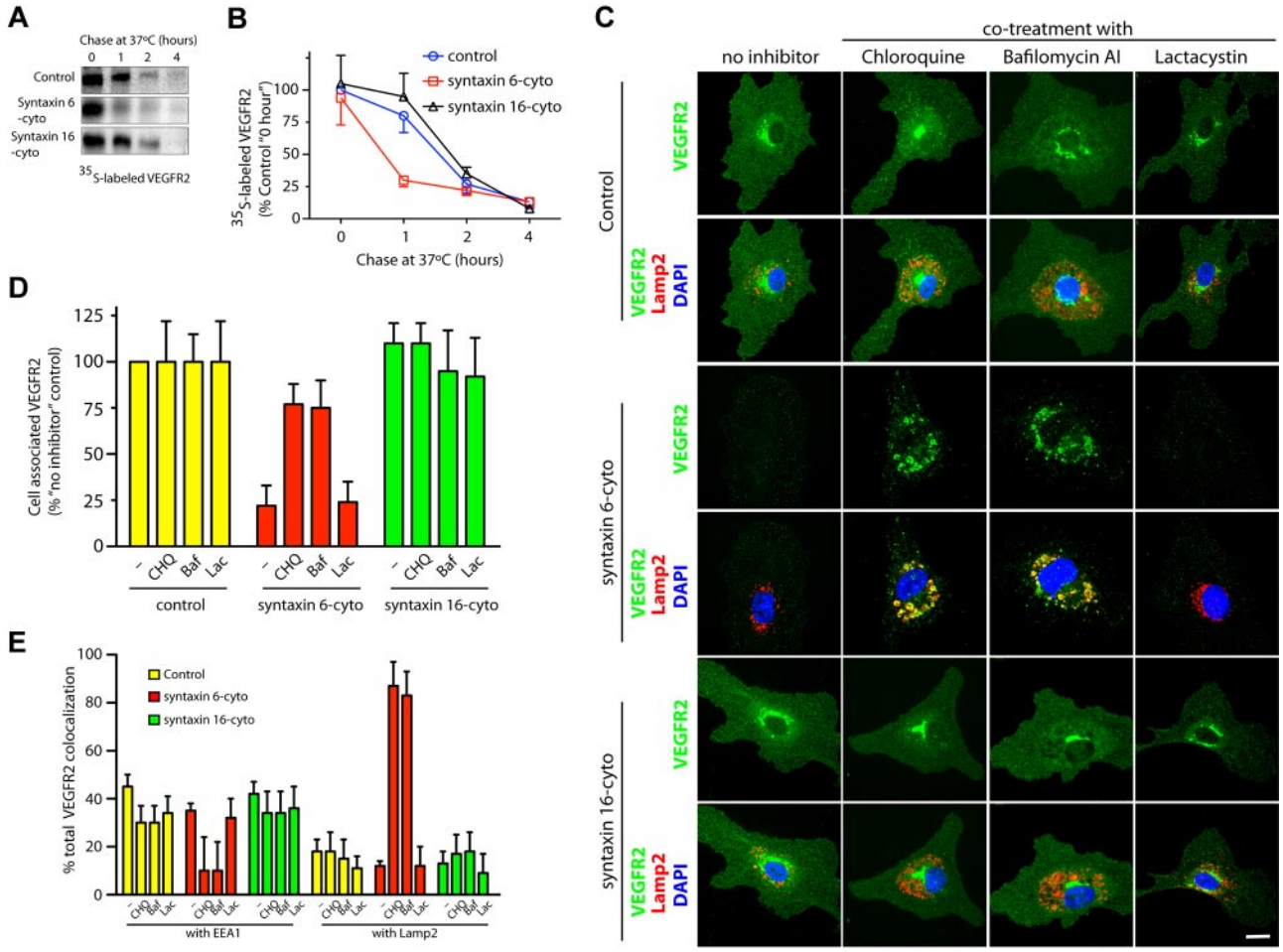

Figure 3. Inhibition of syntaxin 6 function targets VEGFR2 to the lysosomes for degradation. (A,B) Uninfected (Control) and syntaxin 6-cyto– or syntaxin 16-cyto–infected HUVECs (20 hours of infection) were metabolically labeled with ^{35}S-methionine–^{35}S-cysteine for 20 minutes. After the indicated chase period in an excess of unlabeled methionine-cysteine, the cells were lysed and total cell-associated precipitated. Radioactive counts were normalized before immunoprecipitation with VEGFR2 antibody (55B11). Autoradiographic signals from films were measured using Image J software Version 1.38x (NIH) and are represented as a percentage of the time 0 values for uninfected controls. Values are mean (± SD) for n = 3; $P \leq .05$. (C,E) After 18 hours of infection, uninfected (Control) and syntaxin 6-cyto– or syntaxin 16-cyto–treated HUVECs were incubated for an additional 6 hours in complete medium (with 0.05% dimethyl sulfoxide [control], 100μM CHQ, 100nM Baf, or 5μM Lac). Samples were then costained with antibodies against VEGFR2, EEA1 (data not shown), or Lamp2 and observed by fluorescence microscopy. Fluorescence images were used to quantitate total cell-associated VEGFR2 (D) or the colocalization of VEGFR2 with EEA1 or Lamp2 (E). Values in panels D and E represent mean (± SD) for n = 80 cells for each condition from 5 separate experiments; $P \leq .05$. Scale bar represents 5 μm.

significant decrease in colocalization between syntaxin 6 and VEGFR2 at the Golgi (colocalization dropping from 95% to 55%), with a concomitant increase in colocalization in endosomes (from 10% to 40%, supplemental Figure 3A,C). These results suggest that syntaxin 6 may contribute to the regulation of VEGFR2 trafficking at either Golgi or endosomal locations.

To determine whether transport of VEGFR2 from the ER to the Golgi is essential for subsequent receptor transport from the Golgi to the cell surface, we applied brefeldin A (BFA, a fungal metabolite that disrupts the Golgi structure and blocks ER to Golgi protein transport[32]) to HUVECs. This resulted in a redistribution of the VEGFR2 pool from the perinuclear Golgi to vesicular structures distributed throughout the cytosol (Figure 1F). Cell-surface biotinylation revealed that a 30-minute BFA treatment reduced cell-surface VEGFR2 by 80% relative to levels in untreated controls (Figure 1G-H). Notably, BFA treatment (30 minutes) did not result in a change in the total cellular levels of VEGFR2 (Figure 1G). These results suggest that disrupting membrane transport from the ER to the Golgi complex blocks cell-surface delivery of VEGFR2.

Functional inhibition of the Golgi-localized t-SNARE syntaxin 6 leads to a decrease in the cellular pool of VEGFR2

Syntaxin 6, syntaxin 10, and, syntaxin 16 all localized predominantly to the Golgi apparatus based on colocalization with trans-Golgi network marker TGN46 (supplemental Figure 2). We next inhibited the function of these syntaxins by expressing the inhibitory, cytosolic domains of syntaxin 6, syntaxin 10, and syntaxin 16 (designated as syntaxin 6-cyto, syntaxin 10-cyto, and syntaxin 16-cyto, respectively).[18,24] In the case of syntaxin 6-cyto and syntaxin 16-cyto, 95% or more of the HUVECs expressed the cytosolic inhibitory form after 24 hours of infection (supplemental Figure 4A). This overexpression had no effect on morphology of the Golgi apparatus, as ascertained by TGN46 staining (supplemental Figure 4B). Furthermore, overexpression of syntaxin 6-cyto has been shown previously not to affect other SNARE proteins.[18]

The effects of overexpressing syntaxin 6-, syntaxin 10-, or syntaxin 16-cyto on the cellular distribution and level of the VEGFR2 was evaluated by epifluorescence microscopy and Western blot analysis (Figure 2 and supplemental Figure 6A).

Overexpression of syntaxin 6-cyto resulted in significantly altered total cellular levels of VEGFR2 (Figure 2A,D). Western blotting revealed that total levels of VEGFR2 were decreased to 25% of pretreatment levels after 24 hours of syntaxin 6-cyto infection, and to 10% after 36 hours (Figure 2E-F). In contrast, syntaxin 6-cyto infection did not alter the distribution or overall cellular levels of VEGFR1 relative to those in untreated control cells or in cells treated with syntaxin 16-cyto (Figure 2C-D). Overexpression of EGFP-syntaxin 10–cyto and EGFP-syntaxin 16–cyto had no effect on the cellular distribution or levels of VEGFR2 relative to those in untreated control cells (Figure 2 and supplemental Figure 6). These studies were complemented by the use of siRNAs targeting endogenous *STX6* and *STX16*, and a short hairpin RNA targeting *STX10*, to knock down these proteins; in all cases, protein levels were diminished by 90% or more after 72 hours (supplemental Figures 5-6). In the case of siRNAs against *STX6* or *STX16*, the efficiency of knockdown was assessed by immunofluorescence microscopy. The fraction of HUVECs showing a 90% or greater reduction in syntaxin 6 or syntaxin 16 levels after siRNA treatment was 12% to 15% (supplemental Figure 5). Knockdown of syntaxin 6 in HUVECs using an siRNA against syntaxin 6 led to a 75% reduction in cellular VEGFR2 (Figure 2B,D). From these results, we conclude that syntaxin 6 function is required specifically for maintaining a normal level of VEGFR2, but not for maintaining a normal level of VEGFR1.

Functional inhibition of syntaxin 6 leads to targeting of VEGFR2 to lysosomes for degradation

We next examined the consequences of syntaxin 6 inhibition on VEGFR2 turnover in HUVECs. Pulse-chase experiments were performed to determine the effects on synthesis and stability of newly synthesized VEGFR2. The amounts of newly synthesized VEGFR2 in cells expressing syntaxin 6-cyto or syntaxin 16-cyto were similar to those in untreated controls (ie, at 20 minutes pulse and 0 minutes chase; Figure 3A). After 1 hour of chase, however, syntaxin 6-cyto expressing cells showed a 75% or greater reduction in VEGFR2 relative to initial levels (Figure 3A-B). This expression was not mirrored in syntaxin 16-cyto expressing cells, in which the extent of degradation at this time was less than 10% and even lower than that in uninfected control cells ($< 25\%$). During longer chase periods (2 hours and 4 hours), the extent of receptor degradation in syntaxin 6-cyto or syntaxin 16-cyto expressing cells was similar to that in untreated control cells. These results suggest that inhibiting syntaxin 6 function does not lead to inhibition of VEGFR2 synthesis, but rather to more rapid degradation of the newly synthesized pool of receptor.

We next determined whether syntaxin 6-cyto–induced VEGFR2 degradation occurs in lysosomes or proteasomes. After 18 hours of treatment with either syntaxin 6-cyto or syntaxin 16-cyto, cells were treated with CHQ, an inhibitor of lysosomal hydrolases,[33] with Baf, an inhibitor of the vacuolar-type H^+-ATPase,[34] or with Lac, an inhibitor of the proteasome[35] for an additional 6 hours. We then examined the cellular distribution of VEGFR2 by epifluorescence microscopy. As expected, syntaxin 6-cyto expressing cells that had not been treated with an inhibitor showed significantly reduced VEGFR2 staining. However, syntaxin 6-cyto expressing cells incubated with either CHQ- or Baf-accumulated VEGFR2 in enlarged perinuclear, Lamp2-positive lysosomes (Figure 3C). Quantification of epifluorescence images revealed that the intensity of staining for total cellular VEGFR2 in syntaxin 6-cyto expressing cells was reduced to 25% of that in untreated control cells (Figure 3D). Cotreatment of infected syntaxin 6-cyto cells with CHQ or Baf partially rescued VEGFR2 levels ($\sim 80\%$) to that of the levels seen in untreated control cells (Figure 3D). Incubation with the proteasomal inhibitor Lac did not rescue syntaxin 6-cyto–induced degradation of VEGFR2 (Figure 3C-D). Quantitation of total VEGFR2 colocalization in syntaxin 6-cyto expressing cells with markers for early endosomes (EEA1) or lysosomes (Lamp2) revealed a greater than 85% overlap with Lamp2, and a less than 10% overlap with EEA1 (Figure 3E). The intracellular distribution of VEGFR2 in syntaxin 16-cyto expressing cells treated with various inhibitors was similar to that seen in control cells. These data show that inhibition of syntaxin 6 function leads to the targeting of VEGFR2 to lysosomes for degradation.

Functional inhibition of syntaxin 6 does not lead to the targeting of PM-localized VEGFR2 for degradation

VEGF binding to cell surface VEGFR2 leads to the internalization and subsequent sorting of receptors for degradation in lysosomes.[5] We sought to understand whether syntaxin 6 inhibition targets the PM pool of VEGFR2 for degradation. 2 different approaches to label the PM pool of VEGFR2 were used: surface biotinylation and ScFv antibody binding. In the case of surface biotinylation, cells were subjected to a 16°C temperature block, during which surface-biotinylated VEGFR2 could bind VEGF, internalize, and accumulate in endosomes. After unbound surface biotin was removed (this was considered the initial amount of biotinylated VEGFR2), cells were subjected to a 37°C chase (Figure 4A). After 30 minutes, cell-associated–biotinylated VEGFR2 in control and syntaxin 16-cyto–treated cells decreased to 5% to 10% of the initial levels (Figure 4A-B). Although the amount of biotinylated VEGFR2 in syntaxin 6-cyto expressing cells was lower than in control cells (0 minute chase), a subsequent chase at 37°C did not further decrease the biotinylated pool of receptors relative to initial levels (Figure 4A-B). In the complimentary antibody-binding approach, we labeled surface VEGFR2 using ScFv, which recognizes the extracellular domain of VEGFR2.[25] Cell-surface binding of ScFv was lower in syntaxin 6-cyto expressing cells than in control and syntaxin 16-cyto expressing cells (Figure 4C-D). This reduction in cell-surface ScFv antibody binding could have been because of a reduction in the total cellular level of VEGFR2 as a consequence of syntaxin 6-cyto expression, as shown in Figure 2D. The cells were then subjected to a 16°C temperature block followed by a chase at 37°C. After 30 minutes the intracellular levels of remaining cell-associated ScFv were decreased to 12% of the initial levels in control and syntaxin 16-cyto expressing cells (Figure 4C,E). In syntaxin 6-cyto expressing cells, however, the level of cell-associated antibody was not decreased relative to the initial levels (Figure 4C,E). These results show that in the absence of syntaxin 6 function, the cell-surface pool of VEGFR2 is not targeted for degradation in the lysosomes.

Functional inhibition of syntaxin 6 blocks VEGF-induced endothelial cell proliferation and migration

To study the functional significance of inhibiting syntaxin 6 in HUVECs, we evaluated VEGF-induced cell proliferation in cells treated with syntaxin 6-cyto or syntaxin 16-cyto. We found that the expression of syntaxin 6-cyto, but not that of syntaxin 16-cyto, blocked cell proliferation in response to VEGF (Figure 5A). Thus, trafficking of VEGFR2 to the endothelial cell-surface by a syntaxin

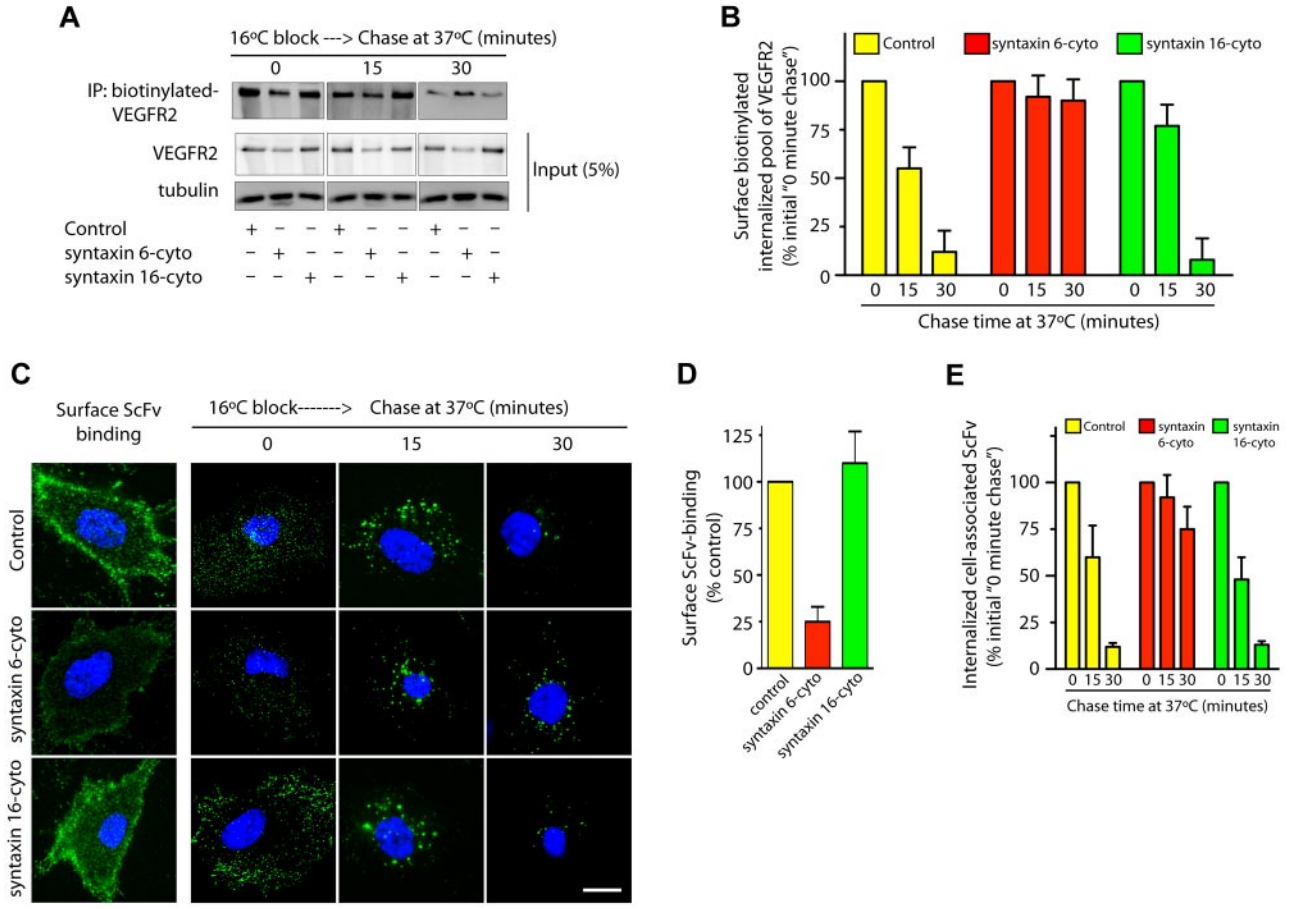

Figure 4. Syntaxin 6 inhibition does not target endocytic pool of VEGFR2 for degradation. (A-E) Serum-starved uninfected (Control) and syntaxin 6-cyto or syntaxin 16-cyto infected HUVECs (20 hours of infection). (A-B) Cells were surface biotinylated as described for Figure 1F. Samples were then incubated at 16°C for 30 minutes to allow biotinylated VEGFR2 to accumulate in endosomes. The remaining surface biotin was removed by treatment with sodium 2-mercaptoethanesulfonate (MesNa) and quenching of MesNa with iodoacetic acid. These samples (0-minute chase time point) were further incubated at 37°C for the indicated periods. To determine the levels of intracellular biotinylated VEGFR2 after different chase periods, cells were again treated with MesNa to remove any additional biotinylated VEGFR2 that had recycled to the cell surface. Intracellular biotinylated VEGFR2 was pulled down by streptavidin-Sepharose as described for Figure 1F. Levels of intracellular biotinylated VEGFR2 were quantitated by immunoblotting for VEGFR2. Total cell lysates were also immunoblotted with the indicated antibodies to assess relative protein abundance. (B) Densitometric analysis of immunoblots in panel A. Values are expressed relative to 0-minute chase time point (normalized to 100%). Values are presented as mean (± SD) for n = 3, $P \leq .05$. (C,D) HUVECs were labeled with an E-tagged anti-VEGFR2 antibody (ScFv), at 10°C for 30 minutes, and then incubated with VEGF for an additional 30-minutes. Cells were washed and imaged to assess ScFv-binding at the cell surface. Samples in which ScFv was bound to the cell surface were further incubated at 16°C for 30 minutes. The remaining surface-bound antibody was removed by washing with low pH buffer. These samples (0-minute chase time point) were subjected to chase at 37°C in the presence of VEGF. Cell surface–localized and internalized ScFv-VEGFR2 complexes were detected using an FITC-conjugated antibody against the E-tag. (D,E) Graphs represent quantitative measurements of cell surface–localized and total internalized VEGFR2, as determined by image analysis. Values in panel E are expressed as the percentage of total internalized ScFv fluorescence at the 0-minute chase time point. Values in panels D and E represent mean (± SD) for n = 90 cells for each condition from 3 separate experiments, $P \leq .005$. Scale bar represents 5μm.

6–dependent mechanism is critical for VEGF-induced endothelial cell proliferation.

The impact of inhibiting syntaxin 6 on cell motility was examined in a scratch-wound assay in which endothelial cell motility depends on VEGF (Figure 5B-C). In untreated cells, VEGF treatment for 24 hours led to a 3-fold increase in the migration of cells into the wounded area. However, this effect was significantly suppressed by the expression of syntaxin 6-cyto. The expression of syntaxin 16-cyto did not repress endothelial cell migration relative to levels in uninfected controls. We further examined the role of syntaxin 6 in directional endothelial cell migration using the Boyden chamber assay. As shown in Figure 5D, the expression of syntaxin 6-cyto inhibited the migration of cells toward the chemoattractant VEGF: in uninfected control cells, VEGF stimulated cell migration by between 2- and 2.5-fold, but it had no effect on migration in syntaxin 6-cyto expressing cells (Figure 5D).

We next investigated the role of syntaxin 6 in endothelial tube formation by examining the effect of syntaxin 6 manipulation on endothelial cell morphogenesis within the extracellular matrix. In uninfected cells, tubular structures formed within 6 hours of seeding the cells on Matrigel. The addition of VEGF significantly enhanced tube formation, leading to an increase in the number of intercellular contacts and in the overall complexity of the network (Figure 5E). The expression of syntaxin 6-cyto clearly suppressed this VEGF-induced response, whereas the expression of syntaxin 16-cyto did not (Figure 5E-F). Overall, these in vitro results suggest that functional syntaxin 6 is required to elicit a VEGF-induced chemotactic and mitogenic effect in endothelial cells.

Inhibition of syntaxin 6 and $VEGF_{164}$-induced angiogenesis

Because it was found that $VEGF_{164}$ induces angiogenesis in mouse ears, we next investigated the effects of the inhibitory form of syntaxin 6 on vascularization in a mouse ear model of angiogenesis.[36] Intradermal administration of adenoviral (Ad)–$VEGF_{164}$ led to initiation of angiogenesis by day 3 after injection, and had a robust effect by day 5. This angiogenic response mimics the

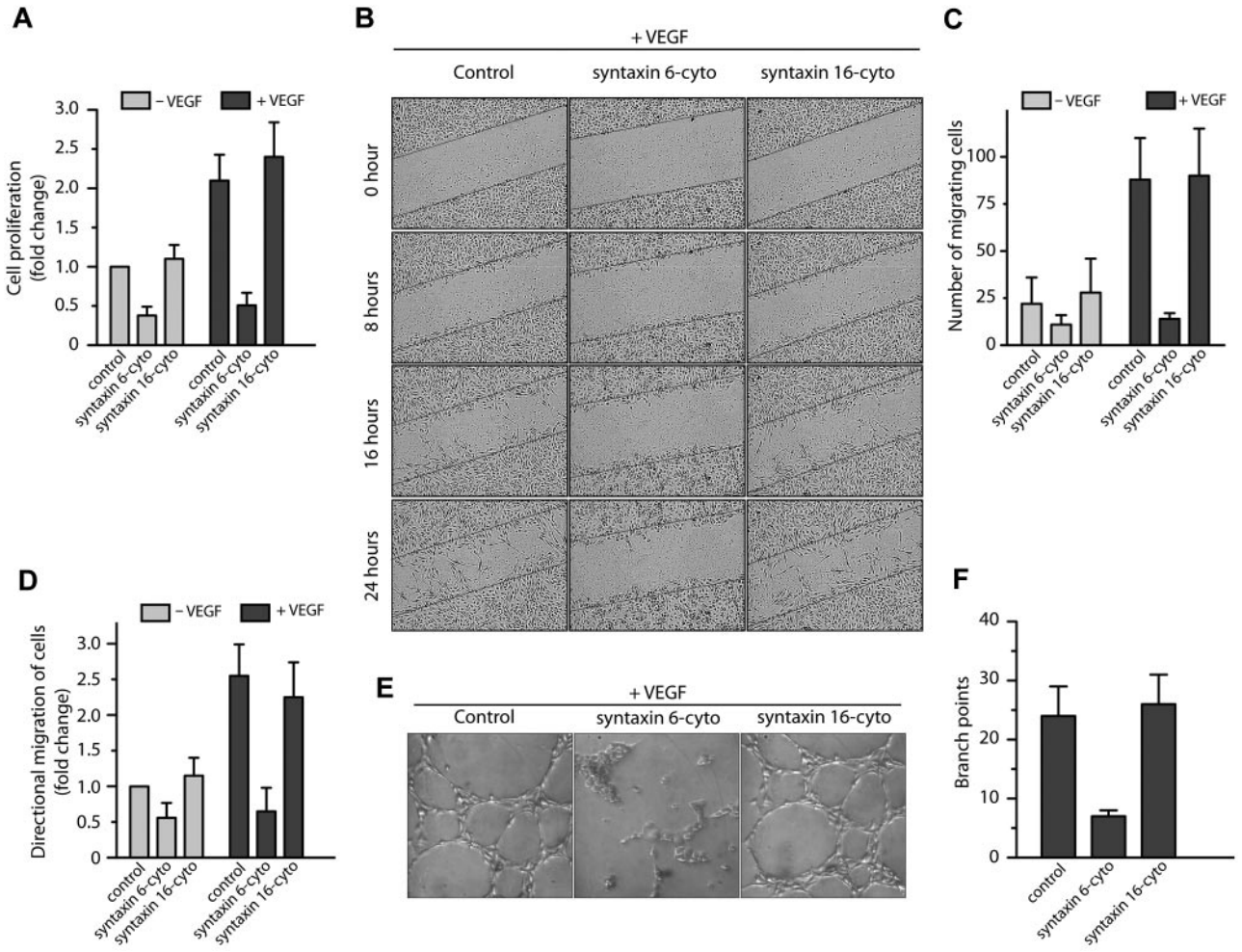

Figure 5. Inhibition of syntaxin 6 blocks VEGF-induced cell proliferation, migration and, morphogenesis in Matrigel. (A,E) Serum-starved HUVECs were left uninfected (Control) or were infected with syntaxin 6-cyto or syntaxin 16-cyto. (A) Cell proliferation assays were carried out using the MTT (3-[4,5-dimethylthiazol-2-yl]-2,5-diphenyltetrazolium bromide) assay. Values are expressed as fold change relative to that in controls. (B) Wound healing in the presence or absence (data not shown) of VEGF as monitored by time-lapse imaging for a period of 24 hours. The wound edges are marked by a solid black line. (C) Quantification of the number of cells migrating into the wound. (D) Directional migration of HUVECs toward VEGF (100 ng/mL) by Boyden chamber assay, with VEGF present in the lower well. The number of migrating cells was normalized to that in unstimulated control cells. (E-F) Matrigel-based tube-formation assay was carried out with HUVECs in the presence of VEGF (100 ng/mL). The number of tubes per field was quantified. Data in panels A, C, D, and F are mean (± SD) from 4 independent experiments. $P \leq .001$ in panel A, $P \leq .005$ in panel C, and $P \leq .05$ in panels D and F.

pathologic angiogenesis mediated by VEGF.[37] The scheme described in Figure 6A was used to evaluate whether the expression of syntaxin 6-cyto in mouse ears would reduce angiogenesis after $VEGF_{164}$ stimulation. Intradermal injection of syntaxin 6-cyto or syntaxin 16-cyto 2 days before injection of Ad-$VEGF_{164}$, followed by the preparation of tissue lysates from angiogenic areas, revealed the expression of inhibitory cytosolic forms of syntaxin 6 or syntaxin 16 (Figure 6B). In mice mock-injected with phosphate-buffered saline (PBS), the level of $VEGF_{164}$ after 5 days of the administration of Ad-$VEGF_{164}$ was increased approximately 12-fold (Figure 6C). In cohorts injected with syntaxin 6-cyto or syntaxin 16-cyto, a similar level of $VEGF_{164}$ expression was observed in ear tissues. In the absence of $VEGF_{164}$, injection of syntaxin 16-cyto and syntaxin 6-cyto did not have a significant effect on the vasculature (data not shown). Upon subsequent administration of Ad-$VEGF_{164}$, a robust increase in vascularity and edema was observed in the ears of mice treated with PBS or syntaxin 16-cyto (Figure 6D-E). However, in syntaxin 6-cyto–treated ears, we noted a marked attenuation of the angiogenic and tissue edema responses under the same conditions (Figure 6D-E). Immunohistochemical staining with CD31 and VEGFR2 showed that syntaxin 6-cyto–infected mouse ears formed only few new vessels in response to $VEGF_{164}$ relative to their mock- or syntaxin 16-cyto–injected counterparts (Figure 6F-G). VEGF-A is a potent vascular permeability factor that induces hemorrhage and extravasation of an intravascular dye (Evans blue) in the mouse ear model.[29] Notably, in Evans blue dye-based analysis of the vasculature in ears similarly treated with Ad-$VEGF_{164}$, the vasculature of syntaxin 6-cyto injected mouse ears showed little dye infusion compared with that in the mock- or syntaxin 16-cyto–injected animal ears (Figure 6H-I). These in vivo results show that the expression of an inhibitory form of syntaxin 6 blocks VEGF-induced angiogenesis and permeability in mouse ear tissue.

Discussion

The abundance of VEGFR2 at the PM is determined by the activities of several intracellular receptor trafficking pathways.[38] These include the pathways that affect the following: secretory transport (for newly synthesized receptor), internalization, activation, lysosomal degradation, and recycling to the PM. Before the

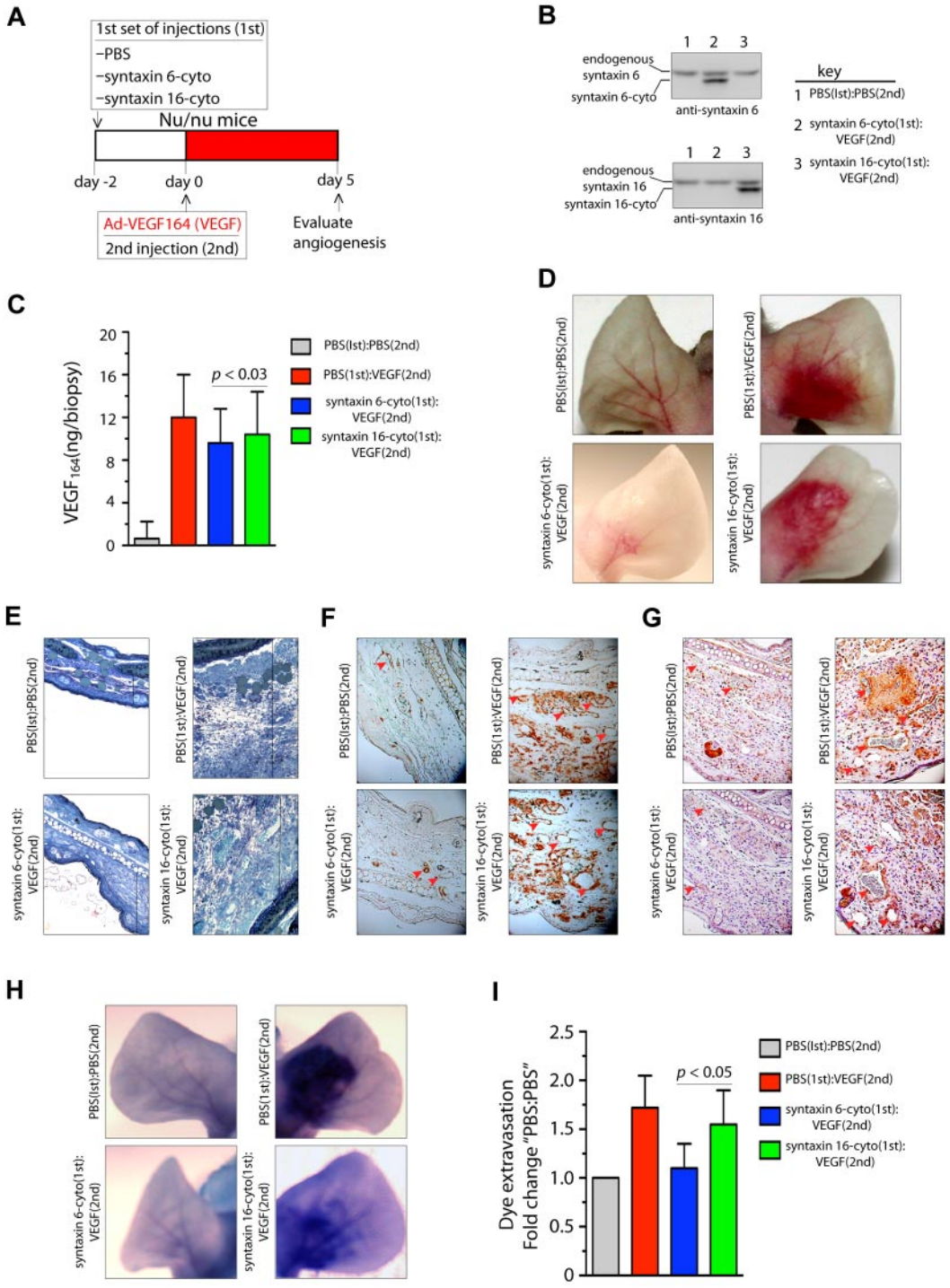

Figure 6. Expression of syntaxin 6-cyto in mice blocks $VEGF_{164}$-induced angiogenesis and permeability. (A,G) Mice in each group (all of which were Nu/Nu mice) were given 2 injections under anesthesia. The first set of injections (1st) was PBS, syntaxin 6-cyto, or syntaxin 16-cyto. The second (2nd) was PBS or Ad-$VEGF_{164}$, and given 2 days later at the site of first injection as shown in panel A. At 7 days after the first set of injections, animals were euthanized and the ears were either photographed or removed for further processing. (B) Western blot analysis of syntaxin 6-cyto and syntaxin 16-cyto expression in mouse ear lysates prepared 5 days after Ad-$VEGF_{164}$ treatment as described in panel A. (C) Quantification of $VEGF_{164}$ levels in ear extracts using the Quantikine Mouse VEGF immunoassay kit (R&D Systems). Values represent mean (± SD) for n = 10 ears, $P \leq .005$). (D) Representative images showing gross appearance of angiogenesis in mock, syntaxin 6-cyto– or syntaxin 16-cyto–injected mouse ears, 5 days before Ad-$VEGF_{164}$ administration. (E,G) Ears were collected and processed for detailed histologic assessment. (E) Representative images showing staining of 1-μm Epon spur sections stained with Toludine blue. Vertical line marks extent of edema developed after different treatments. (F-G) Immunohistochemical staining of mouse ear sections stained with antibodies against CD31 (F) or VEGFR2 (G). Red arrowheads mark blood vessels developed after different treatments. (H,I) In an experiment similar to that described in panel C, mice treated 5 days before with Ad-$VEGF_{164}$, were injected with Evans blue dye. (H) Mouse ears were photographed 30 minutes after injection, and representative images are shown. (I) Quantification of dye extravasation, carried out in another group of mice that were euthanized. Ears were removed and Evans blue dye was extracted and measured spectrophotometrically. Quantitated values represent mean (± SD) for n = 10 ears per data point, $P \leq .03$.

current study, little was known regarding secretory transport of VEGFR2 from the Golgi apparatus to the PM. Our findings demonstrate that a significant amount of VEGFR2 is present in the Golgi apparatus, and that VEGF mobilizes this pool from the Golgi compartment. Moreover, using 2 different loss-of-function approaches, we show that maintenance of intracellular levels of VEGFR2 requires the Golgi- and endosome-localized t-SNARE syntaxin 6. Our findings further reveal that inhibition of syntaxin 6 function leads to targeting of the Golgi-localized, but not the PM-localized, pool of VEGFR2 for degradation in lysosomes. Importantly, inhibiting syntaxin 6 also had tangible effects on cellular processes involved in VEGF-induced angiogenesis. Based on these findings, we propose a model in which the Golgi- and endosome-localized pool of the t-SNARE syntaxin 6 contributes to the regulation of proper VEGFR2 sorting, thereby promoting VEGFR2 turnover at the PM and subsequent angiogenesis (supplemental Figure 1).

VEGFR2 internalizes via a clathrin-dependent pathway, and the endocytic pool of receptors can recycle both constitutively and in response to VEGF stimulation.[5,10] VEGF stimulation also leads to sorting of a fraction of the internalized endocytic pool of VEGFR2 for degradation in the lysosomes. In this study, we report that in unstimulated cells approximately 25% of total VEGFR2 is localized in the Golgi apparatus and cofractionates with the Golgi marker TGN46 by density gradient centrifugation. We also show that VEGF stimulates exit of VEGFR2 from the Golgi, probably by coupling cell-surface VEGFR2-mediated signaling with trafficking from the Golgi. Our results with BFA, which blocks ER-Golgi transport of cargo molecules, show that the total levels of VEGFR2 remain unaltered and that it is only the level of receptor at the cell surface that is reduced, suggesting that secretory transport of VEGFR2 through the Golgi complex plays an important role in maintaining the surface pool of VEGFR2 in endothelial cells.

Syntaxin 6 localizes primarily to the trans-Golgi network and endosomes, suggesting that this t-SNARE plays a role in trans- or post-Golgi fusion events.[23,30,31] This demonstration is consistent with our previous work that syntaxin 6 regulates post-Golgi transport of the membrane microdomain-associated glycosylphosphatidylinositol-green fluorescent protein in human fibroblasts,[18] as well as with other studies showing that syntaxin 6 participates in the maturation and/or exocytosis of granules in specialized cell types[22] and that it is vital to the transport of cargo to the lysosomes in pancreatic beta-cells.[19] For example, syntaxin 6 is involved in a membrane-trafficking step that sequesters the glucose transporter Glut4 away from the PM[20] and recycles insulin-responsive aminopeptidase from the PM back to the insulin-responsive compartment.[39] Syntaxin 6 is also required for the sorting of proteins from endosomes to either the trans-Golgi network or lysosomes.[19] Syntaxin 6 is a component of the cystic fibrosis transmembrane conductance regulator (CFTR)–associated ligand (CFTR-binding protein, CAL) complex in which context it contributes to regulation of the intracellular levels and function of CFTR.[40] In the present study we found that inhibiting syntaxin 6 function results in a reduction of VEGFR2 levels in endothelial cells. It has been previously shown that stimulation with VEGF targets a fraction of the endocytic pool of VEGFR2 for degradation in lysosomes. Given that blockers of lysosome function, but not inhibitors of proteasome function, reversed VEGFR2 down-regulation in response to syntaxin 6, it appears that inhibiting syntaxin 6 function leads to VEGFR2 targeting to the lysosomes for degradation. Our study and findings from published reports[19] suggest that the PM/endocytic pool of VEGFR2 is not likely the target of this lysosome-mediated degradation in the context of syntaxin 6 dysfunction. Indeed we found that only the Golgi-associated pool of VEGFR2 was affected. Our data support the hypothesis that syntaxin 6 is required for maintenance of the Golgi pool of VEGFR2, and that in the absence of syntaxin 6 this pool of receptors is targeted to lysosomes for degradation. However, whether VEGFR2 is targeted directly from the Golgi complex to lysosomes, or instead makes this journey via endosomes, remains to be explored.

VEGFR2 is critical for angiogenesis in pathologic as well as physiologic contexts. Binding of VEGF to VEGFR2 induces receptor activation and thereby endothelial cell proliferation, migration, survival, and tube formation during neovascularization.[41-43] The reduction in VEGF-induced proliferation, migration, and tube formation, we observed in culture upon inhibiting syntaxin 6 function confirms that syntaxin 6 plays a pivotal role in maintaining cellular VEGFR2 levels and angiogenesis. These findings suggest that syntaxin 6-regulated trafficking of VEGFR2 is vital to each of these processes in endothelial cells. Moreover, the physiologic relevance of these findings is strongly supported by our analysis of the consequences of interfering with syntaxin 6 function (via adenoviral gene transfer of syntaxin 6-cyto) with respect to VEGF-induced vascularization (ear assay in nude mice). Finally, our finding that expressing a cytosolic form of syntaxin 6 blocks VEGF-induced angiogenesis raises the prospect that pharmacologic manipulation of syntaxin 6 function in the setting of vascular disorders may be an effective therapeutic tool. During angiogenesis the VEGFR2 signaling cascades can be modulated by additional endothelial cell-surface proteins such as neuropilin-1 and EphrinB2.[44-46] Moreover, inhibition of neuropilin-1 function has been shown to enhance the effectiveness of anti-VEGF therapy in tumor models.[44] In addition, EphrinB2 has recently been shown to regulate VEGFR2 signaling by modulating receptor trafficking from the cell surface.[45,46] It is thus possible that the observed in vivo antiangiogenic effect after sytnaxin 6 inhibition may be dependent on additional cell-surface regulators of angiogenesis that are capable of modulating VEGF-signaling. Future studies investigating the effects of cell type–specific ablation of syntaxin 6 in the tissue microenvironment will more clearly delineate the role of this t-SNARE in angiogenesis.

In summary, we have provided the first demonstration that the t-SNARE syntaxin 6 is involved in maintenance of the intracellular levels and distinct pools of VEGFR2 in the Golgi complex and endosomes. Furthermore, we have shown through our experiments in the mouse model that the cytosolic inhibitory form of syntaxin 6 has antiangiogenic properties.

Acknowledgments

We thank Dr John Engelhardt for providing resources for purifying recombinant adenoviruses, and Dr Robert Tomanek for help with endothelial cell tube formation assay. We also thank Sarah Bloomberg for technical assistance and acknowledge Dr Christine Blaumueller for editorial contributions.

This work was supported by NIH grants R01HL089599 (A.C.), R01CA127958 (A.G.), and R01HL70567 and R01CA78383 (D.M.), as well as by funding from the Carver Foundation at the University of Iowa (A.C.).

Authorship

Contribution: V.M. performed in vitro experiments; A.T. performed in vitro and animal experiments; J.-J.J. performed in vitro experiments; R.B. conducted wound healing and animal experiments; A.G. conducted Boyden chamber migration assays and analyzed the results; D.M. designed the mouse ear angiogenesis assay and analyzed the data; and A.C. designed the study, performed in vitro experiments, analyzed the data, and wrote the manuscript.

Conflict-of-interest disclosure: The authors declare no competing financial interests.

Correspondence: Amit Choudhury, PhD, Department of Anatomy & Cell Biology, University of Iowa, 51 Newton Rd, Iowa City, IA 52242; e-mail: amit-choudhury@uiowa.edu.

References

1. Leung DW, Cachianes G, Kuang WJ, Goeddel DV, Ferrara N. Vascular endothelial growth factor is a secreted angiogenic mitogen. *Science.* 1989; 246(4935):1306-1309.
2. Waltenberger J, Claesson-Welsh L, Siegbahn A, Shibuya M, Heldin CH. Different signal transduction properties of KDR and Flt1, two receptors for vascular endothelial growth factor. *J Biol Chem.* 1994;269(43):26988-26995.
3. Olsson AK, Dimberg A, Kreuger J, Claesson-Welsh L. VEGF receptor signaling: in control of vascular function. *Nat Rev Mol Cell Biol.* 2006;7(5):359-371.
4. Bruns AF, Herbert SP, Odell AF, et al. Ligand-stimulated VEGFR2 signaling is regulated by coordinated trafficking and proteolysis. *Traffic.* 2010;11(1):161-174.
5. Ewan LC, Jopling HM, Jia H, et al. Intrinsic tyrosine kinase activity is required for vascular endothelial growth factor receptor 2 ubiquitination, sorting and degradation in endothelial cells. *Traffic.* 2006;7(9):1270-1282.
6. Lampugnani MG, Orsenigo F, Gagliani MC, Tacchetti C, Dejana E. Vascular endothelial cadherin controls VEGFR-2 internalization and signaling from intracellular compartments. *J Cell Biol.* 2006;174(4):593-604.
7. Salikhova A, Wang L, Lanahan AA, et al. Vascular endothelial growth factor and semaphorin induce neuropilin-1 endocytosis via separate pathways. *Circ Res.* 2008;103(6):e71-79.
8. Jopling HM, Odell AF, Hooper NM, Zachary IC, Walker JH, Ponnambalam S. Rab GTPase regulation of VEGFR2 trafficking and signaling in endothelial cells. *Arterioscler Thromb Vasc Biol.* 2009;29(7):1119-1124.
9. Lanahan AA, Hermans K, Claes F, et al. VEGF receptor 2 endocytic trafficking regulates arterial morphogenesis. *Dev Cell.* 18(5):713-724.
10. Gampel A, Moss L, Jones MC, Brunton V, Norman JC, Mellor H. VEGF regulates the mobilization of VEGFR2/KDR from an intracellular endothelial storage compartment. *Blood.* 2006; 108(8):2624-2631.
11. Ferrara N, Kerbel RS. Angiogenesis as a therapeutic target. *Nature.* 2005;438(7070):967-974.
12. Allan BB, Balch WE. Protein sorting by directed maturation of Golgi compartments. *Science.* 1999;285(5424):63-66.
13. Glick BS, Malhotra V. The curious status of the Golgi apparatus. *Cell.* 1998;95(7):883-889.
14. Mellman I, Simons K. The Golgi complex: in vitro veritas? *Cell.* 1992;68(5):829-840.
15. Pelham HR, Rothman JE. The debate about transport in the Golgi–two sides of the same coin? *Cell.* 2000;102(6):713-719.
16. Chen YA, Scheller RH. SNARE-mediated membrane fusion. *Nat Rev Mol Cell Biol.* 2001;2(2):98-106.
17. Hong W. SNAREs and traffic. *Biochim Biophys Acta.* 2005;1744(3):493-517.
18. Choudhury A, Marks DL, Proctor KM, Gould GW, Pagano RE. Regulation of caveolar endocytosis by syntaxin 6-dependent delivery of membrane components to the cell surface. *Nat Cell Biol.* 2006;8(4):317-328.
19. Kuliawat R, Kalinina E, Bock J, et al. Syntaxin-6 SNARE involvement in secretory and endocytic pathways of cultured pancreatic beta-cells. *Mol Biol Cell.* 2004;15(4):1690-1701.
20. Perera HK, Clarke M, Morris NJ, Hong W, Chamberlain LH, Gould GW. Syntaxin 6 regulates Glut4 trafficking in 3T3-L1 adipocytes. *Mol Biol Cell.* 2003;14(7):2946-2958.
21. Wang Y, Tai G, Lu L, Johannes L, Hong W, Tang BL. Trans-Golgi network syntaxin 10 functions distinctly from syntaxins 6 and 16. *Mol Membr Biol.* 2005;22(4):313-325.
22. Wendler F, Page L, Urbe S, Tooze SA. Homotypic fusion of immature secretory granules during maturation requires syntaxin 6. *Mol Biol Cell.* 2001;12(6):1699-1709.
23. Wendler F, Tooze S. Syntaxin 6: the promiscuous behaviour of a SNARE protein. *Traffic.* 2001;2(9): 606-611.
24. Proctor KM, Miller SC, Bryant NJ, Gould GW. Syntaxin 16 controls the intracellular sequestration of GLUT4 in 3T3-L1 adipocytes. *Biochem Biophys Res Commun.* 2006;347(2):433-438.
25. Grazia Lampugnani M, Zanetti A, Corada M, et al. Contact inhibition of VEGF-induced proliferation requires vascular endothelial cadherin, beta-catenin, and the phosphatase DEP-1/CD148. *J Cell Biol.* 2003;161(4):793-804.
26. Chen TT, Luque A, Lee S, Anderson SM, Segura T, Iruela-Arispe ML. Anchorage of VEGF to the extracellular matrix conveys differential signaling responses to endothelial cells. *J Cell Biol.* 188(4):595-609.
27. Sharma DK, Choudhury A, Singh RD, Wheatley CL, Marks DL, Pagano RE. Glycosphingolipids internalized via caveolar-related endocytosis rapidly merge with the clathrin pathway in early endosomes and form microdomains for recycling. *J Biol Chem.* 2003; 278:7564-7572.
28. Bhattacharya R, Senbanerjee S, Lin Z, et al. Inhibition of vascular permeability factor/vascular endothelial growth factor-mediated angiogenesis by the Kruppel-like factor KLF2. *J Biol Chem.* 2005; 280(32):28848-28851.
29. Nagy JA, Feng D, Vasile E, et al. Permeability properties of tumor surrogate blood vessels induced by VEGF-A. *Lab Invest.* 2006;86(8):767-780.
30. Bock JB, Klumperman J, Davanger S, Scheller RH. Syntaxin 6 functions in trans-Golgi network vesicle trafficking. *Mol Biol Cell.* 1997;8(7):1261-1271.
31. Simonsen A, Gaullier JM, D'Arrigo A, Stenmark H. The Rab5 effector EEA1 interacts directly with syntaxin-6. *J Biol Chem.* 1999;274(41):28857-28860.
32. Klausner RD, Donaldson JG, Lippincott-Schwartz J. Brefeldin A: insights into the control of membrane traffic and organelle structure. *J Cell Biol.* 1992; 116(5):1071-1080.
33. Smith RM, Jarett L. Ultrastructural basis for chloroquine-induced increase in intracellular insulin in adipocytes: alteration of lysosomal function. *Proc Natl Acad Sci U S A.* 1982;79(23):7302-7306.
34. Yoshimori T, Yamamoto A, Moriyama Y, Futai M, Tashiro Y. Bafilomycin A1, a specific inhibitor of vacuolar-type H(+)-ATPase, inhibits acidification and protein degradation in lysosomes of cultured cells. *J Biol Chem.* 1991;266(26):17707-17712.
35. Fenteany G, Standaert RF, Lane WS, Choi S, Corey EJ, Schreiber SL. Inhibition of proteasome activities and subunit-specific amino-terminal threonine modification by lactacystin. *Science.* 1995;268(5211):726-731.
36. Pettersson A, Nagy JA, Brown LF, et al. Heterogeneity of the angiogenic response induced in different normal adult tissues by vascular permeability factor/vascular endothelial growth factor. *Lab Invest.* 2000;80(1):99-115.
37. Nagy JA, Dvorak AM, Dvorak HF. VEGF-A and the induction of pathologic angiogenesis. *Annu Rev Pathol.* 2007;2:251-275.
38. Scott A, Mellor H. VEGF receptor trafficking in angiogenesis. *Biochem Soc Trans.* 2009;37(Pt 6):1184-1188.
39. Watson RT, Hou JC, Pessin JE. Recycling of IRAP from the plasma membrane back to the insulin-responsive compartment requires the Q-SNARE syntaxin 6 but not the GGA clathrin adaptors. *J Cell Sci.* 2008;121(Pt 8):1243-1251.
40. Cheng J, Cebotaru V, Cebotaru L, Guggino WB. Syntaxin 6 and CAL mediate the degradation of the cystic fibrosis transmembrane conductance regulator. *Mol Biol Cell.* 21(7):1178-1187.
41. Ferrara N. Vascular endothelial growth factor: basic science and clinical progress. *Endocr Rev.* 2004;25(4):581-611.
42. Ferrara N, Gerber HP, LeCouter J. The biology of VEGF and its receptors. *Nat Med.* 2003;9(6):669-676.
43. Matsumoto T, Claesson-Welsh L. VEGF receptor signal transduction. *Sci STKE.* 2001;2001(112): re21.
44. Pan Q, Chanthery Y, Liang WC, et al. Blocking neuropilin-1 function has an additive effect with anti-VEGF to inhibit tumor growth. *Cancer Cell.* 2007;11(1):53-67.
45. Sawamiphak S, Seidel S, Essmann CL, et al. Ephrin-B2 regulates VEGFR2 function in developmental and tumour angiogenesis. *Nature.* 465(7297):487-491.
46. Wang Y, Nakayama M, Pitulescu ME, et al. Ephrin-B2 controls VEGF-induced angiogenesis and lymphangiogenesis. *Nature.* 465(7297):483-486.